International Journal of Advanced Research in Physical Science (IJARPS)
Volume 6, Issue 5, 2019, PP 20-28
ISSN No. (Online) 2349-7882
www.arcjournals.org

What would be Inside of M87* to Explain the VHT Results

Stefan Mehedinteanu*

Center of Technology and Engineering for Nuclear Projects Atomistilor no. 409, Bucharest-Magurele, Romania

Corresponding Author:** ***Stefan Mehedinteanu, *Center of Technology and Engineering for Nuclear Projects Atomistilor no. 409, Bucharest-Magurele, Romania*

Abstract: *The holographic entanglement via bit threads flux lines it could be viewed as the common cause for almost of cosmic Universe epochs, as Electroweak Phase Transition (EWPT), CMBR and Confinement, others events like Black holes (BHs) merging and the lensing effects. The bit threads (magnetic flux lines) are produced in the bulk of bodies as due of the EWPT bubbles collisions that being filed with a Higgs field, and quarks-gluons in case of nucleons. All the known parameters of M87* Event Horizon Telescope Results are explained in terms of these new models.*

1. Introduction

From " First M87 Event Horizon Telescope Results" [1], we can extract the followings:"The horizon-scale emission of M87 at 1.3 mm exhibits a robust crescent-like structure.The global very long baseline interferometry (VLBI) at an observing wavelength of 1.3mm (230 GHz) with Earth-diameter-scale baselines is required to resolve the shadows of the core of M87.

The crescent morphology, rapid drop to a deep interior flux depression, and broad consistency among days, methods, and the stellar dynamics measurement all point to the emission structure from M87 being due to strong gravitational lensing around a central black hole.

VLBI observations at 1.3mm have revealed a diameter of the emission region of $\cong 40\mu as \cong 1.2\times 10^{12}[m]$, which is comparable to the expected horizon-scale structure. Finally, the radio core in M87 is quite typical for powerful radio jets in general.

This measurement from lensed emission near the event horizon is consistent with the presence of a central Kerr black hole, as predicted by the general theory of relativity.

In [1] they present in Section 3 a pedagogical description showing how within compact ring models the emission diameter and central flux depression (shadow) can be inferred

directly from salient features of the visibility data" .

In some refs cited in [1], is shown that "in many Active galactic nuclei (AGNs), collimated relativistic plasma jets (Bridle &Perley 1984; Zensus 1997) launched by the central black hole contribute to the observed emission. These jets may be powered either by magnetic fields threading the event horizon, extracting the rotational energy from the black hole (Blandford & Znajek 1977), or from the accretion flow (Blandford &Payne 1982). The near-horizon emission from low-luminosity active galactic nuclei (LLAGNs); Ho 1999) is produced by synchrotron radiation that peaks from the radio through the far infrared. This emission may be produced either in the accretion flow (Narayan et al. 1995), the jet (Falcke et al. 1993), or both (Yuan et al. 2002) ".

In [1] the appearance of M87* has been modeled successfully using general-relativistic

Magnetohydrodynamics (GRMHD) simulations, which describe a turbulent, hot, magnetized disk orbiting a Kerr black hole. They naturally produce a powerful jet and can explain the broadband spectral energy distribution observed in LLAGNs. At a wavelength of 1.3 mm, and as observed here, the simulations also predict a shadow and an asymmetric emission ring.

In my opinion, from these models do not result the cause of shadow of the BH, and by what mechanism is transformed the matter accretion flow into near-horizon emission.

In the following we will come with a new model in the spirit of more common physical raisons used in cosmology, as a combination of, the inflation, the electroweak phase transition (EWPT) Universe epoch (~100GeV~0.1m), when the BH is viewed as spacetime region, the origin and the content of black holes [BHs), FLRW, the entanglement holograms, all being experienced by the author himself in recent works, in order to explain the Earth lensing, the CMBR appearance and frequency, LIGO strain, etc. [15÷18], and the companion references mentioned therein, and repeated here.

2. The Gravito-Electric Einstein Tensor in Core of BH

In the case of a homogeneous potential directed along the z-axis [10] eq. (2.2), the Einstein stress-energy tensor is:

$$T^{00}=T^{11}=T^{22}=-T^{33}=\rho=\frac{\varepsilon_0 c^2 B^2}{8\pi};\ T^{0i}=0, \tag{1}$$

where $\rho_B[J/m^3]$-the magnetic energy density.

$$\varepsilon=\frac{V_{vol}\varepsilon_0 c^2 B^2}{8\pi}=\rho V_{vol}=V[J], \tag{2}$$

$V_{vol}=2\pi\lambda_C\lambda_c(4\lambda_C)\cong 8\pi\lambda_C^3$, at Compton length equally with the penetration length $\lambda_C=\lambda$, that results

$$E^2=\frac{(V)}{\varepsilon_0(\lambda_C^{e*})^3} \tag{3}$$

With $V=\varepsilon_{gluons}$ as above is obtained $B=E_{q\bar{q}}/c$.

$$\varepsilon=\frac{V_{vol}\varepsilon_0 c^2 B^2}{8\pi}=\rho_B V_{vol}=V=m_A=[J], \tag{4}$$

$V_{vol}=2\pi\lambda_C\lambda_c(4\lambda_C)\cong 8\pi\lambda_C^3$, at Compton length $\lambda_C=\eta/mc$

$$E^2=\frac{(V)}{\varepsilon_0(\lambda_C^{e*})^3}\quad \text{, also } E=Bc=\frac{\eta c}{e\lambda_C^2} \tag{5}$$

Here, the Hubble constant is defined as

$$H^2=\frac{1}{R_{Earth}^2}=\frac{8\pi GV^4}{3(\eta c)^3 c^4}\rightarrow\frac{8\pi GV^4}{3\lambda_C^3(mc^2)^3c^4}\rightarrow\frac{8\pi G}{3}\frac{V}{\lambda_C^3 c^4}[m^{-2}] \tag{6}$$

Or based on bit-threads [15÷18] as

$$\frac{c^3\cdot\rho\cdot l_P^2}{3\eta}\frac{1}{c^2}=H^2[m^{-2}] \tag{7}$$

$$\rho\big|_{bulk}=n_{bit\_threads}\rho_{bubble}=n\rho=n\frac{T_j}{c^2\lambda_C^3}$$

For example, $\rho=\dfrac{M_U}{n_{bit\_threads}\cdot\lambda_C^3\cdot a_{end}^2}$; (8)

$n=n_{bit\_threads}=\dfrac{M_U c^2}{m_A\cdot a_{end}}$; the Compton length $\lambda_C=\eta/m_A c$

Since the quarks inside BHs, as commoving particles following the collisions of the Electroweak (EW) bubbles filled with Higgs field, generate an electromagnetic field (EM) by a pulsating process [12] with frequency $v=\omega^{-1}$, a such pulse of stress-energy it could be $8\pi T_{\mu\nu}k^\mu k^\nu=a\delta(\lambda)$, a is a positive constant, and the surface gravity $\kappa=\frac{c^3}{GM}[s^{-1}]$.

We can observe that $\frac{\Delta A}{A}=\frac{8\pi GM}{c^2}\cdot\frac{1}{R}=\frac{r_{Schw}}{R}$, or, we have obtained the classical formula for deformation.

3. MAGNETIC FIELD GENERATION IN FIRST ORDER PHASE TRANSITION BUBBLE COLLISIONS

When the Universe supercooled below the critical temperature ($T_c \approx 100GeV$) the Higgs field locally tunneled from the unbroken $SU(2) \times U(1)_Y$ phase to the broken $U(1)_{em}$ phase [5].

The tunneling gave rise to the formation of broken phase bubbles which then expanded by converting the false vacuum energy into kinetic energy.

The typical size of a bubble after the phase transition is completed is in the range

$$R_{bubble} \sim f_b H_{EW}^{-1} \quad (9)$$

Where

$$H_{EW}^{-1} \sim \frac{m_{Pl}}{g_*^{1/2} T_c^2} \approx 10cm \quad (10)$$

is the size of the event horizon at the electroweak scale, m_{Pl} is the Planck mass, $g_* \sim 10^2$ is the number of massless degrees of freedom in the matter, and the fractional size f_b is $\sim 10^{-2} \div 10^{-3}$.

Törnkvist in [5], discusses the suggestion made in cited Ref. [9], that magnetic fields may be generated in the decay of Z -strings. It is well-known that the unstable Z -string decays initially through charged W -boson fields. The idea is that these W fields form a “condensate” which then in turn would act as a source of magnetic fields. The conventional gauge-invariant definition of the electromagnetic field tensor in the

SU(2) × U(1) Yang-Mills-Higgs system is given by following eq. where

a possible generalization of the definition for the Weinberg-Salam model was given by Vachaspati [5]. It is conceivable, however, that the large conductivity of the plasma in the early universe, cited refs. [2, 1, 33] may cause the magnetic field lines to freeze into the fluid so that it remains preserved at later times.

To note also, that, in case of electroweak and QGP epochs the magnetogenesis is analyzed for different mechanisms [15÷18]

We can now wonder what is the strength of the magnetic fields at the end of the EWPT. A partial answer to this question has been recently given in [19] where the formation of ring-like magnetic fields in collisions of bubbles of broken phase in an abelian Higgs model were inspected.

Under the assumption that magnetic fields are generated by a process that resembles the Kibble and Vilenkin [24] mechanism, when W condensate- and Zstrings-configurations are expected to form, it was concluded that a magnetic field is of the order $B = 2 \times 10^{20} G \cong 2 \times 10^{16} [T]$.

Assuming turbulent enhancement of the field by inverse cascade, a root-mean-square value of the magnetic field $B_{rms} = 10^{-21} G \cong 10^{-17} [T]$ on a commoving scale of $10Mpc \cong 3 \times 10^{23} [m]$ as from [11].

In the case of a first order electroweak phase transition, the Higgs field inside a given bubble has an arbitrary phase [19]. The bubbles expand and eventually collide, while new bubbles are continuously formed, until the phase transition is completed. This also involves the equilibration of the phases of the complex Higgs fields, the gradients

of which act as a source for gauge fields, thus making the generations of magnetic fields possible. The magnetic field generated in bubble collisions will be imprinted on the background plasma.

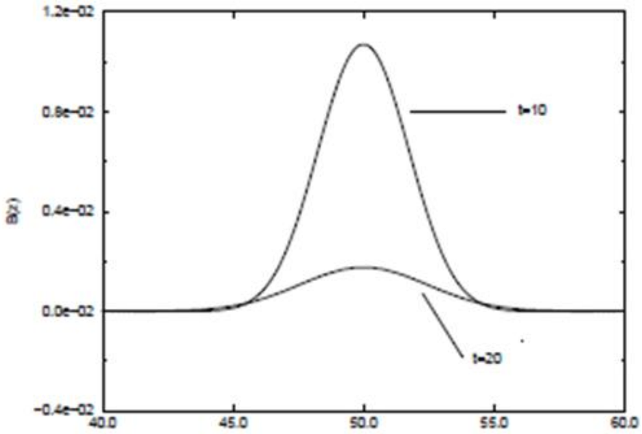

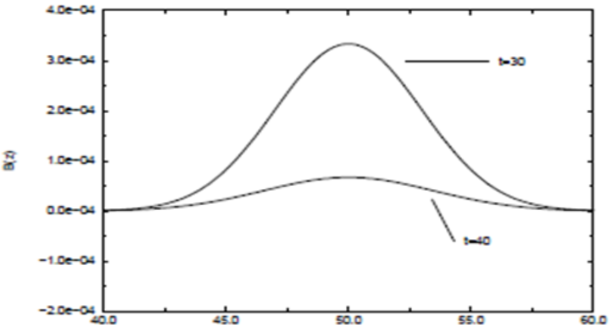

Figure 5 from [19]: B with v = 1, r = 1, σ = 7, R = 10 and t = 10, 20, 30 and 40 after the initial collision. The point of initial collision on the z-axis is $z_1 = 50$ (and units are $e\eta = 1$; the gauge boson mass $m_A = "e\eta" = T_c$).

It is convenient to write the Higgs field in polar form:

$\Phi = \frac{1}{\sqrt{2}} X e^{i\theta}$; X settles rapidly to its equilibrium value η.

Again the magnetic field escapes from the bubbles intersection region and moves outwards with the speed of light.

4. The Born Of Pairs Inside the Bubbles as Permanent Process

Now, the rate per unit volume of pairs creation is given by using the Schwinger effect R inside the EW bubbles $R = (E/E_{cr})^2 (c/\lambda^4)(8\pi^3)^{-1} * \exp(-\pi E_{cr}/E)$ (11)

or $E/E_{cr} << 1$, , mass m, and so-called “critical” electric field

$E_{cr} = m^2 c^3 / e\eta$

the volume is given by:

$V_{matter} = (\lambda_C)^4 \frac{1}{c}[m^3 s]$; m -the mass of pairs $(W^{\pm}, q^{\pm})$.

5. The Strain at Event Horizon

From [12] we have:

$\lambda = \kappa^{-1} e^{\kappa v}$; $\kappa^{-1} = 4M$; $v = t + r^*$; $C = 1 - 2M/r$; and $r^* = \int C^{-1} dr$; $C_{,r} = 2M/r^2$

We will assume that $T_{vv}(v)$ represents ingoing radiation which changes the black hole’s mass by only a small fractional amount, $|\Delta M| << M$. We can then take κ to be constant to lowest order. If we change the independent variable from λ to v = t + r∗, then

$\frac{d}{d\lambda} = e^{-\kappa v} \frac{d}{dv}$; $v = 1/\omega$; $\kappa = \frac{c^3}{4GM}$

And

$T_{\mu\nu} k^{\mu} k^{\nu} = e^{-2\kappa v} T_{vv}$

For spherically symmetric pulses, the shear and vorticity vanish, and the Raychaudhuri equation, Eq. (36) from [12], becomes

$$\frac{d\theta}{dv} = -\frac{1}{2} e^{\kappa v} \theta^2 - 8\pi e^{-\kappa v} T_{vv}(v)$$

The equation for the horizon area can be expressed as

$$\frac{dA}{dv} = e^{\kappa v} A\theta$$

If we take $A_0 = 16M_0^2$ to be the initial area of the black hole in the distant past, where M_0 is its initial mass, then we have

$$\frac{\Delta A}{A_0} \cong \frac{a}{\kappa} e^{\kappa v_+} = 2\frac{\Delta M}{M_0}$$

In this approximation, the change in the mass of the black hole is

$$\Delta M = \frac{a}{2\kappa} M_0 e^{\kappa v_+} = \frac{aA_0}{8\pi} e^{\kappa v}$$

where we have used $\kappa = 1/(4M) \cong 1/(4M_0)$.

This agrees with the result obtained by calculating the change in mass directly from Eq. (12) as $\dot{M} = \frac{dM}{dt} = F = \int T_t^r r^2 d\Omega$

Here, it was defined an "effective magnetic field", B_{eff}, in terms of the total energy density in the magnetic field of MF Vortex,

$$\varepsilon_0 = \frac{\varepsilon_0 c^2 B_{eff}^2}{8\pi} \qquad (12)$$

On the horizon, $T_t^r = T_{vv}$, $r = 2M + \varepsilon$

Since the quarks generated inside nucleons or in EW bubbles are generated by a pulsating process with frequency $v = \omega^{-1}$, a such pulse of stress-energy it could be $8\pi T_{\mu\nu} k^\mu k^\nu = a\delta(\lambda)$, a is a positive constant, and the surface gravity $\kappa = \frac{c^3}{GM}[s^{-1}]$.

We can observe that $\frac{\Delta A}{A} = \frac{8\pi GM}{c^2} \cdot \frac{1}{R} = \frac{r_{Schw}}{R}$, or, we have obtained the classical formula for deformation.

6. The Pre-Formation of BH at EWPT Universe Epoch

First step-at EWPT epoch

$\varepsilon_{EWPT} = 100GeV \to 1.7\times10^{-8} J$; $a_{end-EW} = 0.9$; $k_{end}^{-1} = 0.1[m]$, with eq. (6), (7) results $R = 0.4m$ and eq. (8) for $\rho = 4\times10^{28}[kg/m^3]$, or $H_{end}^{-1} = 0.1 \cong H_{EW}^{-1}[m]$, $t_{end} = H_{end}^{-1}/c = 3.3\times10^{-10} s$, $n_{bit\_threads} = \frac{M_U c^2}{1.7\times10^{-8}} = 1.1\times10^{64}$; $k_{end}^{-1} = 0.1$; $B_{EWPT} = 7.7\times10^{18}[T]$; $\lambda_C = 1.7\times10^{-18}$; $H_{leave}^{-1} = k_{leave}^{-1} = 10^{-18}[m]$ we found $N = 39.22$

At BH spacetime

From [1], the mass of M87 is appreciated as $M_U = 10^9 \times M_{SUN} = 1.98\times10^{39} Kg$,and with $\varepsilon_{BH} = 100/a_{end\_BH} = 7\times10^{-3} GeV = 1.12\times10^{-12} J$, when, the initially $m_A \cong 100GeV$ at 0.1 m, at commoving distance of BH diameter this becomes $m_A = 7MeV \to B_{magnetic\_flux=} = 3.26\times10^{10}[T]$, from eq. (5), that corresponds with quarks mass. As a rule, the build of spacetime is obtained by using well-known Inflation models as in A.H.Guth [13], $k_{end} = H_{leave}^{-1} e^N [m^{-1}]$; $a_{end} = k_{end}^{-1}/H^{-1}$; $H_{leave} = 0.1[m]$; $N(\varphi)$ -e- folds, thus the horizon-entry is when $k_{end} = k_{leave} e^{-N}$; $k_{end}^{-1} = 3.5\times10^7[m]$, $a_{end\_BH} = 1.43\times10^4$, and with eq. (6), the spacetime deformation Becomes $H_{end}^{-1} = R = 1.1\times10^{10}[m]$, and respectively, from eq. (7) with $\rho = 4.6\times10^7[kg/m^3]$ from eq. (8), also $H_{end}^{-1} = 5.5\times10^9[m]$; when the number of bit-threads as above is $n = n_{holog\,ram} = 1.1\times10^{64}$; $t_{end} = H_{end}^{-1}/c \cong R/c = 1670[s]$, $T = 8.3\times10^{10}[K]$, with $H_{leave}^{-1} = k_{laeve}^{-1} = 0.1[m]$ we found $N = 19.675$ to match the iterations cycle: $m_g \to \eta v \to k_B T \to \varepsilon \to R \to H_{end}^{-1} \to a_{end} \to N$. $\lambda_{C\_BH} = 2.67\times10^{-14}[m]$ the curvature radius R is equally with Schwarzschild radius $r_{sch} = 2.9\times10^{12}[m]$

at BH diameter

, and with $\varepsilon_{near} = 0.01/a_{end\_near} = 7\times10^{-3} GeV = 1.12\times10^{-12} J$, at commoving distance of BH diameter $m_A = 7MeV \rightarrow B_{magnetic\_flux=} = 3.25\times10^{10}[T]$, with eq. (5), the horizon-entry is when $k_{end} = k_{leave}e^{-N}$; $k_{end}^{-1} = 5\times10^{11}[m]$, $a_{end\_near} = 1$, and with eq. (6), $H_{end}^{-1} = 1.1\times10^{8}[m]$, and respectively near the same with eq. (7) for $\rho = 6.6\times10^{11}[kg/m^3]$ from eq. (8), and the number of bit threads is $n = n_{ho\log ram} = 1.1\times10^{68}; r_{object} \approx r_{Sch}$, $t_{end} = H_{end}^{-1}/c \cong R/c = 1673[s]$, where with $H_{leave}^{-1} = k_{laeve}^{-1} = 5\times10^{11}[m]$ we found $N = 1.61$ to match the iterations cycle: $m_g \rightarrow \eta\nu \rightarrow k_B T \rightarrow \varepsilon \rightarrow R \rightarrow H_{end}^{-1} \rightarrow a_{end} \rightarrow N$.

$\lambda_{C\_near} = 2.67\times10^{-14}[m]$

at EVT-today

Therefore, the new horizon of EWPT bubbles collisions, where the stress-energy pulse leaves under the form of bit threads, see figure 1., $a_{leave} = k_{leave}/H_{leave} = 1$, or $k_{leave}^{-1} = H_{leave}^{-1} = r_{Schw}$. Now, the new horizon-entry-EVT detector is when the wave length $k_{end} = k_{leave}e^{-N}$; and the scale factor arrives at $a_{end} = k_{end}/H_{end}$, $\varepsilon_{space} = 0.007/a_{end\_space} = 4.73\times10^{-13} GeV = 7.56\times10^{-23} J$ with Compton length $\lambda_C^{EVT-site} = \eta/m_A c = 4\times10^{-4}[m]$; the mass being the same $M_U = 1.9\times10^{39} kg$; $a_{end\_EVT} = 1.48\times10^{10}$ and with eq. (6), the Hubble length $H_{end}^{-1} = 2\times10^{29}[m]$, the same, when the number of bit threads passing through hologram and attaining the EVT-site is $n_{bit\_threads} = \dfrac{M_U c^2}{m_A \cdot a_{end\_EVT}} = 1.06\times10^{58}$, from the total at hologram of $\cong 1.1\times10^{68}$ and from eq. (7) with $\rho = 1.37\times10^{-29}[kg/m^3]$ from eq. (8), it results the today spacetime $H_{end\_space} = 10^{28}[m]$; and for with data for the EVT site, we have the commoving magnetic flux at $B_{magnetic\_flux=} = 1.48\times10^{-10}[T]$, with eq. (5), $t_{end} = H_{end}^{-1}/c = 4\times10^{16} s$, we found $N = 9$ to match the iterations cycle: $m_g \rightarrow \eta\nu \rightarrow k_B T \rightarrow \varepsilon \rightarrow R \rightarrow H_{end}^{-1} \rightarrow a_{end} \rightarrow N$.

In order to identify $e\eta$ in [19], and in figure 5., we proceed as following, we know that for $v = 247GeV \rightarrow \lambda_L^2 = \left(4\pi\alpha v^2/(\eta c)^2\right)^{-1} \cong 5.5e-36m^2$, or $\lambda_L \cong 2.3e-18[m]$, which is the Compton length for $W^{\pm}$ bosons [20]. Thus, we have add one constraint equation to the four Klein-Gordon equations; the only linear, Lorentz invariant choice is $(\Diamond + m^2)A_\mu(x) = 0$ and $\partial_\mu A^\mu = 0$.

$\Diamond = \left(\dfrac{\partial^2}{\partial t^2} - \nabla^2\right)$ is the d'Alembertian. For the time-independent case, the Klein–Gordon equation becomes $\left[\nabla^2 - \dfrac{m^2c^2}{\eta^2}\right]\psi(r) = 0$; where $\dfrac{m^2c^2}{\eta^2} \Leftrightarrow [m^{-2}]$

It then follows that a Klein-Gordon equation holds for A, from [19]

$(\partial_\mu\partial^\mu + e^2\eta^2)X = 0$, where $X = A_\mu$

Introducing $\alpha^{-1} = \dfrac{4\pi\varepsilon_0\eta c}{e^2} = 137$ in λ_L is obtained $\lambda_L^2 = "e^2\eta^2" = \left(\dfrac{e^2v^2}{\varepsilon_0(\eta c)^3}\right)^{-1}$

Therefore, in figure .7 results at the hologram site $"e\eta" = 780[m^{-1}]$; so $50/780 = 0.063[m]$ when $v = m_A/a_{end\_EVT} = 7.56\times10^{-23}[J]$, the same value is obtained if we consider that at EVT site from the number of bit threads of initially value of 10^{68} it pass only $\cong 10^{58}$, in the above formula, we have for the today $v = m_{Anear} \cdot \frac{1.06\times10^{58}}{1.57\times10^{68}} = 7.56\times10^{-23}[J]$, whereas above, also, we have for the pulse dimension as from figure 5., $\cong 50*780 = 3.92\times10^{4}[m^{-1}]$, so the frequency is $\omega = c\cdot"e\eta" = c*780 = 233GHz$, which is in the range of the frequency measured in [1], this being the decisive result which validates the present model.

7. The Hologram and the Spacetime Deformations

Near BH

We use the above model confirmed in others author works [15÷18].

With $a = \frac{c}{R}[s^{-1}]$; where $R = 5\times10^{11}[m]$; $a = 5.9\times10^{-4}$; with $M = 10^{9}\times1.98\times10^{24} = 1.98\times10^{39}[kg]$; $\kappa = 5\times10^{-5}[s^{-1}]$; if we have the generation inside the vacuum of BH as given by eq. (11), $v = \omega^{-1} = (R/V\cdot V_{vol})^{-1}$;where $R/V\times V_{vol} \cong 8.4\times10^{54}\cdot\lambda_C^3 = 1.61\times10^{14}[s^{-1}]$, $\lambda_c = \eta/mc = 2.67\times10^{-14}[m]$; where, the mass of ring's particles (electrons) being $m = 1.25\times10^{-29}[kg]$, that resulting $v = 6.2\times10^{-15}[s]$; and $e^{\kappa v} \cong 1.0$. Here for E we uses eq. (5) , $E = 8.1\times10^{19}[N/C]$, with $V = 1.12\times10^{-12}[J]$ that corresponds to quarks mass, and the magnetic flux is $B = E/c = 3.25\times10^{10}[T]$. Inside the BH this flux is expelled under the form of jets with the frequency ~233 GHz.So, the deformation near BH is $\frac{\Delta A}{A} = 11$; or $\Delta A = 5.48\times10^{9}[m]$, just the BH's core size, or where the lensing is total (the radiation don't escapes), see figure 1.To note that at EWPT epoch the deformation is $\frac{\Delta A}{A} = 5.8\times10^{13}$; or $\Delta A = 10^{13}[m]$ as the spacetime region deformation.

At spacetime-today

With $a = \frac{c}{R}[s^{-1}]$; where $R = 10^{25}[m]$; $a = 2.4\times10^{-17}$; with $M = 10^{9}\times1.98\times10^{24} = 1.98\times10^{39}[kg]$; $\kappa = 5\times10^{-5}[s^{-1}]$; if we have the generation inside the BH as given by eq.(11), $v = \omega^{-1} = (R/V\cdot V_{vol})^{-1}$; where $R/V\times V_{vol} \cong 1.7\times10^{14}\cdot\lambda_C^3 = 10^{4}[s^{-1}]$, $\lambda_c = \eta/mc = 4\times10^{-4}[m]$; where, the mass of ring's particles (electrons) being $m = 8.4\times10^{-40}[kg] \to 7.53\times10^{-23}[J]$, that resulting $v = 9.2\times10^{-5}[s]$; and $e^{\kappa v} \cong 1.0$. Here for E we uses eq. (5) , $E = 0.37[N/C]$, with $V = 7.56\times10^{-23}[J]$ that corresponds to the quarks mass, and the magnetic flux is $B = E/c = 1.48\times10^{-10}[T]$. So, the deformation near BH is $\frac{\Delta A}{A} = 4.9\times10^{-13}$; or $\Delta A = 5\times10^{15}[m]$, or the spacetime deformation is above the ring diameter.In all situations, and in other words, the pulse is expelled from inside BH to holograms.

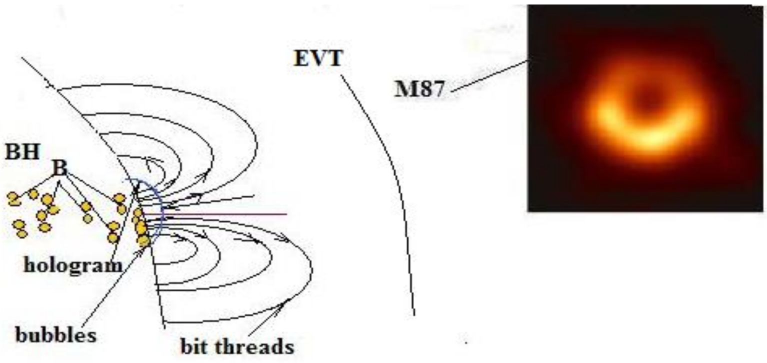

Fig1. *Our model of M87**

8. Conclusion

By using authors developed models, we found that

-M87 it was pre-formed when the spacetime was of 0.1 [m] or at EWPT epoch of Universe as a object of mass $\cong 10^9 \times M_{SUN}$.

-The pulsed EM field it was generated by EWPT bubbles collisions, and at commoving distance of $10^{11} \div 10^{13}$[m] decays to quarks mass.

-The Einstein- stress energy tensor is equally with this field.

-This field is entangled from inside the BH region to the boundary as a hologram, where each particle is a point.

- The flow v by its field lines (also called *flux lines*) with the condition $\nabla \cdot v = 0$ means that the threads cannot begin, end, split, or join in the bulk; each thread can begin and end only on a boundary, which could be the conformal boundary where the field theory lives, or possibly a horizon (e.g. if are considering a single-sided black hole spacetime).

-The hologram is the place of lensing, inside its there is not emission, that gives the shadow (black hole). The field lines passing the hologram give the luminosity with the frequency of 233 GHz as it was calculated, and as being observed by EVT with some bulbs, see figure 1 (left and right).

-The field deforms the spacetime, initially in pre-formation arriving at $r = 10^{13}[m]$ which it remains near constantly till today.

-The rotating body BH (as every cosmic object) being into equilibrium with his ring (the centripetal force equals the gravitational force), the attraction being extend to the deformed spacetime $r = 10^{13}[m]$.

Therefore, again is remarkable the proof of the author models also for this cosmic object.

References

[1] The Event Horizon Telescope Collaboration, First M87 Event Horizon Telescope Results. I. The Shadow of the Supermassive Black Hole, The Astrophysical Journal Letters, 875:L1 (17pp), 2019 April 10

[2] Shawn X. Cui, et al., Bit Threads and Holographic Monogamy, arxiv:1808.05234v1 [hep-th], 2018.

[3] M. Freedman and M. Headrick, Bit threads and holographic entanglement, Commun. Math. Phys. 352, 407 (2017).

[4] T. Faulkner, M. Guica, T. Hartman, R. C. Myers, and M. Van Raamsdonk, Gravitation from entanglement in holographic CFTs, J. High Energy Phys. 03 (2014) 051.

[5] Ola Törnkvist, GINZBURG-LANDAU THEORY OF THE ELECTROWEAK PHASE TRANSITION AND ANALYTICAL RESULTS, arxiv:hep-ph/920.4235v1, 1992.; T. Vachaspati, Phys. Lett. B265 (1991) 258.

[6] Xian-Hui Ge, Can-Can Wang, Emergence of cosmological Friedmann equations from quantum entanglement, arxiv:1709.03290v1 [gr-qc], 2017.

[7] P. Calabrese and J. Cardy, "Entanglement entropy and quantum field theory: A non-technical introduction," [arXiv:quant-ph/0505193].

[8] P. Calabrese and J. Cardy, "Entanglement entropy and quantum field theory," J.Stat. Mech. 0406, P002 (2004) [arXiv:hep-th/0405152]; Entanglement Entropy and Quantum Field Theory, arXiv:hep-th/0405152v3 2 Oct 2008

[9] Shinsei Ryu, Tadashi Takayanagi, Holographic Derivation of Entanglement Entropy from AdS/CFT, arxiv:hep-ph/0603001v2, 2006; arXiv:hep-th/0605073v3, 2006.

[10] Dario Grasso, Hector R. Rubinstein, Potentials in the Early Universe, arxiv:astro-ph/0009061v2, 2001

[11] G. Vidal, J. I. Latorre, E. Rico and A. Kitaev, "Entanglement in quantum critical phenomena," Phys. Rev. Lett.90, 227902 (2003) [arXiv:quant-ph/0211074].

[12] L.H. Ford, Thomas A. Roman, CLASSICAL SCALAR FIELDS AND THE GENERALIZED SECOND LAW, arXiv:gr-qc/0009076v2, 2001.

[13] a) A. H. Guth and S. Y. Pi, Phys. Rev. Lett. 49 (1982) 1110; b) ALAN H. GUTH, Inflation, arxiv:astro-ph/0404546v1 27Apr 2004;

[14] BICEP2 I: DETECTION OF B-mode POLARIZATION AT DEGREE ANGULAR SCALES, arxiv:1403.3985v2[astr-ph.CO] 18Mar 2014.

[15] Stefan Mehedinteanu (Issue 1), On the Nature of CMBR Universe Epoch Hologram, International Journal of Advanced Research in Physical Science (IJARPS) Volume 6, Issue 1, 2019, PP 19-30 ISSN No. (Online) 2349-7882 www.arcjournals.org

[16] Stefan Mehedinteanu (Issue 10), The Lensing Effect a Proof of Large Scale Entanglement in Holographic CFTs, International Journal of Advanced Research in Physical Science (IJARPS) Volume 5, Issue 10, 2018, PP 13-23 ISSN No. (Online) 2349-7882 www.arcjournals.org.

[17] Stefan Mehedinteanu (Issue 11), The Entanglement in Holographic CFTs- an Alternative Explanation of the Binary Black Hole Merger (LIGO) Experiment, International Journal of Advanced Research in Physical Science (IJARPS) Volume 5, Issue 11, 2018, PP 31-42 ISSN No. (Online) 2349-7882 www.arcjournals.org.

[18] Stefan Mehedinteanu, How the Entanglement Hologram Enhances the Nuclear Fusion and the Battery Effect of Light Irradiation of Hydrogen/ Deuterons Layer on Metals and Graphene, International Journal of Advanced Research in Physical Science (IJARPS) Volume 6, Issue 3, 2019, PP 5-23 ISSN No. (Online) 2349-7882 www.arcjournals.org

[19] J. Ahonen and K. Enqvist, Magnetic field generation in first order phase transition bubble collisions, hep-ph/9704334, 1997.

[20] Stefan Mehedinteanu, On the Acceleration of Beta Nuclides Decay by the Photonuclear Reaction, International Journal of Nuclear Energy Science and Engineering (IJNESE) Volume 2, Issue 2 2012 PP. 45-56 www.ijnese.org © World Academic Publishing.

[21] Tsuneo Suzuki, Katsuya Ishiguro, Yoshihiro Mori, Toru Sekido, The dual Meissner effect in SU(2) Landau gauge, arxiv:hep-lat/0410039v1, 2004.

[22] L.S. Kisslinger, hep-ph/0202159

[23] W.B. Kibble and A. Vilenkin, Phys. kin, Phys. Rev. D52 (1995) 679.

Citation: *Stefan Mehedinteanu., (2019). What would be Inside of M87* to Explain the VHT Results. International Journal of Advanced Research in Physical Science (IJARPS) 6(5), pp.20-28, 2019.*